[Frontiers in Bioscience 19, 490-503, January 1, 2014]

Inhibition of macrophage autophagy induced by *Salmonella enterica* serovar typhi plasmid

ShuYan Wu[1], YuanYuan Chu[1], YanRu Yang[1], YuanYuan Li[1], PeiYan He[1], YaJie Zheng[1], Chi Zhang[1], QiuChen Liu[1], Ling Han[1], Rui Huang[1]

[1]*Medical College of Soochow University, No. 199, Ren Ai Road, Suzhou, Jiangsu 215123, P. R. China*

TABLE OF CONTENTS

1. BSTRACT

pR_{ST98}, a chimeric plasmid isolated from *Salmonella enterica* serovar typhi (*S. typhi*), is involved in bacterial multidrug-resistance and virulence, however, its exact contributions to bacterial pathogenesis are still not fully understood. To investigate whether pR_{ST98} exhibits potential to mediate macrophage autophagy and apoptosis, murine macrophage-like cell line (J774A.1) was infected with wild type strain (*S. typhi*-WT), mutant strain (*S. typhi-Delta*pR_{ST98}) and complement of *S. typhi-Delta*pR_{ST98} (*S. typhi*-c-pR_{ST98}). Results revealed that *S. typhi* harboring pR_{ST98} decreased the number of autophagy vacuoles of macrophages as well as the expression of Beclin 1 and LC3-II at the early stage of infection; apoptosis rate of macrophages infected with *S. typhi-Delta*pR_{ST98} was lower than that infected with *S. typhi*-WT or *S. typhi*-c-pR_{ST98}. The survival rate of intracellular bacteria carrying pR_{ST98} was much higher than that of plasmid free strain. After intervention with autophagy agonist rapamycin, apoptosis rate of the cells infected with S. typhi containing pRST98 and intracellular bacterial growth decreased. Our study suggested that pRST98 could inhibit autophagy and induce cell apoptosis for the host bacterial survival and proliferation.

2. NTRODUCTION

Typhoid fever, an ancient infectious disease caused by *Salmonella enterica* serovar typhi (*S. typhi*), is widely recognized as a major cause of infection globally, with an estimated 21 million cases and 200,000 related deaths yearly (1, 2). It has been controlled to some extent in developed countries. However, it remains a serious public health problem in developing countries especially in South and Southeast Asia due to poor sanitation (3-5). In addition, the emergence of drug resistance among *S. typhi* poses major challenges over the last few decades and the possibility of super-resistant *S. typhi* should be alerted *(6, 7)*.

In the late 1980s and early 1990s, a pandemic of multidrug resistant *S. typhi* occurred in P. R. China. Five hundreds and ninety one strains of *S. typhi* were isolated from the blood of patients by our laboratory in Suzhou, and more than 80% of these isolates were multidrug resistant (8, 9). Plasmid profile analysis by our lab indicated that all those multidrug resistant strains carried a 98.6 mDa plasmid designated as pR_{ST98},

which mediates bacterial multidrug resistance to ampicillin (Amp), chloramphenicol (Cm), streptomycin (Sm), trimethoprim (TMP), sulfonamide (Su), gentamicin (Gm), neomycin (Nm), kanamycin (Kn), cephalosporin (Cp), carbenicillin (Cb), and tetracycline (Tc). As described previously, we made the first report that *Salmonella* plasmid virulence (*spv*) homologous genes also existed on pR_{ST98}. The *spv* genes were identified as a highly conserved region of 8 kb with five genes, named *spv*R, A, B, C and D. Further research indicated that pRST98 was associated with the increased virulence in mice, such as lethality, infection of spleen, liver and mesenteric lymph nodes, and serum resistance (8-10). We conclude that pRST98 is a chimeric plasmid both mediating bacterial multidrug resistance and increasing bacterial virulence. However, the mechanism of pRST98-increased bacterial virulence is still poorly illuminated.

Macrophages are important immunocytes that play a pivotal role in innate and adaptive immune systems. They are key players in the immune response to infectious microorganisms, phagocytosing cellular pathogens, controlling bacterial replication by producing anti-microbial molecules, and presenting antigen to stimulate lymphocytes and other immune cells to respond to pathogen. Salmonella is facultative intracellular bacteria that mainly grow and reproduce in the host cells such as macrophages and dendritic cells (DCs) in natural infections. A large body of experimental evidence indicated that residing within macrophages is an essential process for Salmonella to cause systemic infection (11-12). The infected macrophages can transport the replicating intracellular bacteria to the mesenteric lymph nodes and circulation. Salmonella consequently secrete effectors to mediate macrophage apoptosis leading to cell-to-cell spread.

Autophagy is a cellular process that mediates the degradation of long-lived proteins and damaged organelles by delivering them to the lysosomes in the cytosol. It is regulated by nutritional status, hormones and intracellular signalling pathways (13-16). Autophagy has a dual role in intracellular bacterial infection. On one hand, it acts as an important element of host innate and adaptive immunity against bacterial infection (17-19). On the other hand, several intracellular bacteria subvert autophagy and reside within autophagosome-like vacuoles. These bacteria block the fusion of their autophagosome-like compartments with lysosomes; thereby provide a permissive niche for growth (20, 21). *Salmonella* induced autophagy is typically a dynamic, rapid and localized response; thus *Salmonella* infection is considered to be a useful model to study the relationship between autophagy process and the outcome of infectious disease (22, 23). It was known that at least three pathways involved in the activity of autophagy at distinct steps of *Salmonella* infection, including diacylglycerol pathway, galectin-8/NDP52 pathway, and polyubiquitin pathway (17, 24-26). However, strategies for *Salmonella* to evade macrophage autophagy were rarely reported.

To some pathogenic microorganisms, induction of cell death is required for pathogenesis, and apoptosis is the most common strategy. For *Salmonella*, the induction of macrophage apoptosis is a specific virulence mechanism promoting cell-to-cell spread *in vivo*. As reported previously, *S. typhi* harboring pR_{ST98} had the potential to enhance macrophage apoptosis rate and to restrain DCs autophagy (8, 9). However, its exact effect on apoptosis and autophagy in infected macrophages remains elusive. It seems that there are three possible relations between autophagy and apoptosis. Autophagy can serve as the origin of apoptosis, so that inhibition of autophagy may delay the occurrence of apoptosis; autophagy may also antagonize apoptosis, thus inhibition of autophagy will increase the cell sensitivity to apoptosis signals; autophagy participates indirectly in the apoptosis process (27-29). In the present study we showed, for the first time, that pR_{ST98} increased bacterial virulence through inhibiting macrophages autophagy and inducing cell apoptosis.

3. MATERIALS AND METHODS

3.1. acterial strains and culture conditions

Bacterial strains used in this study are listed in Table 1. Those strains were stored at −80°C in phosphate-buffered glycerol. Before adding to cells they were grown to mid-logarithmic phase at 37°C in Luria-Bertani (LB) broth, and quantified spectrophotometrically by determining the optical density at 600 nm along with viable plate counts. Then they were centrifuged at 3,000×*g* for 5 min and resuspended in RPMI 1640 medium.

3.2. Construction of mutant strains

S. typhi-*Δ*pR_{ST98} was pR_{ST98} delete mutation derived from *S. typhi*-WT, which subjected to the curing regiment of growth in LB broth containing 5% sodium salt (SDS). *S. typhi*-WT was passaged daily with low inocula (10^3 to 10^4 CFU) for the curing regiment. When cultures reached in logarithmic growth phase, a portion was diluted and plated on medium without antibiotics. Then cured derivative was acquired by chloramphenicol screening according to its resistance.

Transconjugant strain *S. typhi*-c-pR_{ST98} was constructed by a conjugal transfer of pR_{ST98} to *S. typhi*-*Δ*pR_{ST98}. According to the reference (8, 10), pR_{ST98} was transferred from the *S. typhi*-WT to plasmid-free *Escherichia coli (E. coli)* K12W1485Rif^r F^- Lac^+ (*E. coli* K12W1485); *Shigella* and *Salmonella* selective plates containing rifampicin (100 μg/ml) and chloramphenicol (20 μg/ml) were used to acquire pR_{ST98}/*E. coli* K12W1485. And then pR_{ST98} was transferred from pR_{ST98}/*E.coli* K12W1485 to *S. typhi*-*Δ*pR_{ST98}. Specifically, overnight cultures of the donor and recipient bacteria were prepared in LB broth separately, and then 0.1 ml of each culture were mixed and incubated for 4 h at 37°C, centrifuged at 2,300×*g* for 5 min and resuspended in normal saline. Mixtures were transferred to a LB plate and grown at 37°C overnight. The collected lawn was diluted and spread on selective

Table 1. Strains

	Description	Reference
E. coli K12W1485	$Rif^r F^- Lac^+$	[8]
S. typhi-WT	*spv* $Tc^r Amp^r Cm^r Sm^r Kn^r Cb^r Gm^r Nm^r Su^r TMP^r Cp^r$	[10]
S. typhi-*Δ*pR_{ST98}	*Δspv* $Tc^s Amp^s Cm^s Sm^s Kn^s Cb^s Gm^s Nm^s Su^s TMP^s Cp^s$	This study
S. typhi-c-pR_{ST98}	*spv* $Tc^r Amp^r Cm^r Sm^r Kn^r Cb^r Gm^r Nm^r Su^r TMP^r Cp^r$	This study

r represents resistance and s represents sensitiveness

plates described above. The colonies producing hydrogen sulfide were selected to be cultured on the same selective plates again. After identification of serological and biochemical reactions, extraction and analysis of bacterial plasmid DNA, and PCR amplification of *spv*B and *spv*C genes were performed for further confirmation.

3.3. PCR amplification of *spv*B and *spv*C genes

To insure the construction results of *S. typhi*-*Δ*pR_{ST98} and *S. typhi*-c-pR_{ST98}, *spv*B and *spv*C fragments were amplified by PCR. *E. coli* K12W1485 and *S. typhi*-WT were used as *spv* negative and positive control, respectively. The *spv*B primers were (forward) 5′-ATG TTG ATA CTA AAT GGT TTT TCA-3′ and (reverse) 5′-CTA TGA GTT GAG TAC CCT CAT GTT-3′. The *spv*C primers were (forward) 5′-ATG CCC ATA AAT AGG CCC T-3′ and (reverse) 5′-CTC TGT CAT CAA ACG AT-3′. The conditions for amplification with all primer sets were 95°C for 10 min, followed by 32 cycles of 95°C for 20 s, 55°C for 20 s and 72°C for 1 min, a single extension cycle at 72°C for 5 min. The products were electrophoresed on a 1.2% agarose gel, stained with ethidium bromide and observed under UV light.

3.4. Cell culture and infection

Murine macrophage-like cell line J774A.1 was propagated in RPMI 1640 medium with 10% fetal calf serum at 37°C in a humidified incubator containing 5% CO_2 and 95% free air. Cells from exponentially growing cultures were used in all experiments and seeded in plates for 16-24 h before use. Mid-logarithmic phase growth cultures of *S. typhi*-WT, *S. typhi*-*Δ*pR_{ST98} and *S. typhi*-c-pR_{ST98} were added to J774A.1 macrophages at a multiplicity of infection of 100 bacteria per cell respectively. Bacteria were centrifuged onto cells at 1000×*g* for 10 min at 4°C and cultured at 37°C with 5% CO_2 for 1 h (0-h time point). After washed twice with phosphate-buffer saline (PBS) to remove unbound bacteria, RPMI complete medium containing 100 μg/ml amikacin was added to kill the remaining extracellular bacteria. After 2 h of further incubation at 37°C, the medium in the plates was replaced with RPMI medium containing 10 μg/ml amikacin to prevent extracellular growth of bacteria released from the infected J774A.1 cells. At different time points post infection with bacteria, J774A.1 macrophages were processed in the following methods.

3.5. Plasmid transfection and confocal microscopy detection

J774A.1 macrophages seeded in 24 well-plates with coverslips were transfected with mRFP-GFP-LC3 tandem construction using Lipofectamine 2000 (Invitrogen) for 48 h before infection. After infection, cells were stained with Hoechst 33342 (2 μg/ml, Sigma), fixed with 4% paraformaldehyde in PBS and examined under a confocal laser scanner microscope (TCS-SP2, Leica, Germany). For quantification of punctate LC3 structures, GFP-LC3 and mRFP-LC3 punctated dots were counted in more than 100 cells.

3.6. Detection of the optimal concentration of rapamycin

The cytotoxicity of rapamycin (RAPA) against J774A.1 cells was determined by 3- (4, 5)-dimethylthiahiazo (-z-y1)-3, 5-di-phenytetrazoliumromide (MTT) assay. Cells were seeded into 96-well plates and treated with RAPA under different concentrations at a density of 1×10^4 cells per well. After 12 h incubation, 20 μl of MTT (5 mg/ml, Sigma) was added into each well for 4 h incubation and 150 μl of DMSO was used for 10 min in order to solubilize the blue-purple crystals of formazan afterwards. The absorbance was then measured at 490 nm under a microplate reader (uQuant, Bio-Tek Instruments. Inc., Winooski, VT, USA).

J774A.1 cells were seeded overnight into 24-well tissue culture plates with coverslips. After interacting with RAPA for 12 h, cells were washed twice with PBS, dyed with Giemsa to observe microscopically.

3.7. Preparation of samples for transmission electron microscopy

J774A.1 macrophages were cultured and infected as described above. At the indicated time points post-infection, the adherent cells were scraped with a cell scraper and pelleted by centrifugation. The cells were then fixed with 2.5% glutaraldehyde in 0.1 M phosphate buffer, post-fixed in 1% osmium tetroxide, and dehydrated through a series of graded acetone washes. Samples were embedded in epoxy resin, sectioned, and placed onto 200-mesh copper grids. The grids were stained with uranyl acetate and lead citrate, and samples were examined under transmission electron microscope (H600, Hitachi Co., Japan).

3.8. Assessment of bacterial intracellular survival

For viable count determinations, the infected macrophages were washed three times with PBS at the indicated time points, and bacteria were harvested by adding 1 ml of 0.2% Triton X-100 in dark. After 10 min, cell lysate was collected and serially diluted 10-fold in PBS, and aliquots were plated onto LB agar to enumerate bacterial colony-forming units (CFU).

After infection, cells were stained with Giemsa for counting numbers of intracellular bacteria under light microscope. The numbers of intracellular bacteria were counted in at least 100 infected cells.

3.9. Visible autophagy by immunofluorescence

Infected cells were collected and permeabilized with digitonin (500 μg/ml, Sigma) at room temperature for 5 min, and washed three times with PBS according to the reference (30), with slight modifications. Then cell nuclei were stained with Hoechst 33342 (2 μg/ml, Sigma) for 30 min in dark, and fixed with 70% alcohol for 20 min, similarly washed three times with PBS, incubated with polyclonal rabbit anti-LC3 (1:100, Sigma) for 1 h at room temperature, and washed with PBS, incubated with FITC-conjugated donkey anti-rabbit IgG secondary antibody (1:200, Sigma) for another 1 h. Then samples were washed with PBS, mounted in antifade constituents (10 μl, Beyotime) and viewed under the confocal microscope.

3.10. Assessment of apoptosis and autophagy by flow cytometry

A propidium iodide (PI) apoptosis detection kit (Beyotime) was used to assess the apoptosis of infected J774A.1 macrophages by measuring a typical sub-diploid peak (SD peak) in accordance with the manufacturer's instructions. Cells were pelleted by centrifugation, washed once with ice-cold PBS, and resuspended in 100 μl of Rnase A at 37°C for 30 min. Then, the suspension was incubated with 400 μl of PI for 30 min at 4°C in dark. Finally, the samples were analyzed on a flow cytometer (FC500, Beckman Coulter, Brea, CA, USA). In SD assay, SD peak, appeared in front of diploid DNA peak, represented cells apoptosis, while necrosis cells did not appear SD peak.

Quantification of the LC3-II protein amount was performed using flow cytometry. Cells (1×10^6) were harvested, washed once in PBS and then permeabilized, fixed, incubated with primary and secondary antibody as same as the treatment of immunofluorescence. In each step above, cells were washed three times with PBS and pelleted by centrifugation at 1,000×*g*. Finally, cells were analyzed by flow cytometry to detect mean FITC fluorescence intensity.

3.11. Western blotting analysis of autophagy protein Beclin 1

Western blotting was carried out as follows. Briefly, equal amounts of protein (45 μg) from each sample were loaded into each lane. Proteins were separated by a 12% SDS-polyacrylamide gel electrophoresis, transferred onto a nitrocellulose membrane (Pall Corporation) at 200 mA for 2 h. After blocking with buffer containing 5% nonfat dry milk in Tris-buffered saline, rabbit monoclonal anti-mouse Beclin 1 (1:500, Cell Signaling Technology) was added. Protein detection was performed using a chemiluminescence reagent (ECL, Biological Industries). The visualization was done with Image Quant LAS-4000 (Fujifilm, Tokyo, Japan). Image J launcher broken symmetry software program was applied to quantify the total amount of Beclin 1.

3.12. Assay of caspase-3 activity

After infection with strains for each time point, the J774A.1 cells were collected by centrifugation and washed once with PBS. The cells were then resuspended in lysis buffer and incubated on ice for 30 min. The cell debris was removed by centrifugation at 12,000×g for 10 min at 4°C, and the supernatant was used for the colorimetric assay of caspase-3 activities using commercial kits (Caspase-3 Kit, Beyotime). Para-nitroanilide (*ρ*NA)-conjugated specific substrates were catalyzed by caspase-3 (DEVD-*ρ*NA) according to the manufacturer's instructions. Cleaved substrates *ρ*NA were quantified by reading absorbance at 405 nm with a microplate spectrophotometer. Caspase-3 activity was expressed as the ratio of caspase-3 vitality to the total protein concentration.

3.13. Lactate dehydrogenase assay of cell death

Cell death was quantified by measuring lactate dehydrogenase (LDH) released into the culture medium. LDH activity was estimated using an automated microplate reader by measuring OD value in absorbance at 450 nm following manufacturers' instructions (LDH Assay Kit, Beyotime). LDH release was expressed as the percentage-ratio of LDH release in the medium to total LDH by cell lysate.

3.14 Statistics

All data points represent mean ± standard deviation. All assays were conducted in triplicate and repeated at least three times. Statistical analyses were performed using Student's *t*-test.

4. RESULTS

4.1. Identification for constructed strains

pRST98 existed in *S. typhi*-WT is a chimeric plasmid both mediating bacterial multidrug resistance and virulence. It was cured from *S. typhi*-WT as mutant strain *S. typhi-Δ*pRST98, which received this plasmid again by a conjugal transfer to create *S. typhi*-c-pRST98. Plasmid DNA extraction and analysis was performed according to reference [8]. The electrophoresis assay of plasmid DNA showed that pRST98 was found in *S. typhi*-WT and *S. typhi*-c-pRST98. And it was not found in *S. typhi-Δ*pRST98 and *E. coli* K12W1485 (Figure 1A). Analysis *spv*B (1776 bp) and *spv*C (735 bp) genes, which were always present on pRST98, confirmed availability of all strains as constructed above (Figure 1B and 1C).

4.2. The optimal concentration of rapamycin

MTT assay showed the rate of viable cells under 12.5 μg/ml, 25 μg/ml and 50 μg/ml RAPA treatments were 93%, 89% and 35%, respectively. It indicated that RAPA had little cytotoxicity below 50 μg/ml (Figure 2A). Similarly, results of Giemsa

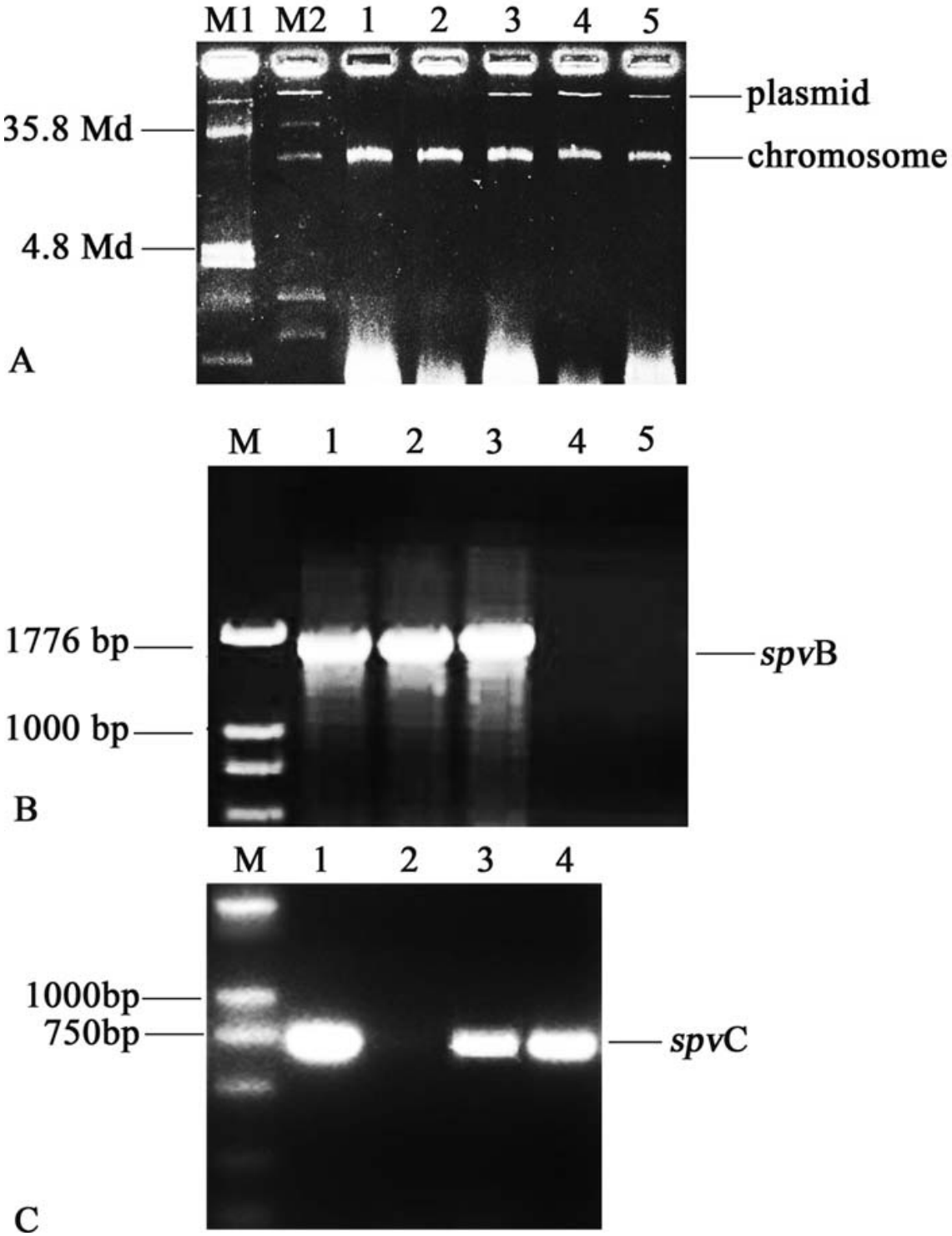

Figure 1. Identification for constructed strains. (A) Plasmid profile of constructed strains. M1: *E. coli* V_{517}, size marker; M2: *S. flexneri*$_{24570}$, size marker; lane 1: *E. coli* K12W1485; lane 2: *S. typhi*-*Δ*pR_{ST98}; lane 3: *S. typhi*-WT; lane 4: pR_{ST98}/*E. coli* K12W1485; lane 5: *S. typhi*-c-pR_{ST98}. (B) PCR amplification of *spv*B (1776 bp) gene. M: Axygen 2000 bp DNA ladder; lane 1: *S. typhi*-WT; lane 2: pR_{ST98}/*E. coli* K12W1485; lane 3: *S. typhi*-c-pR_{ST98}; lane 4: *E. coli* K12W1485; lane 5: *S. typhi*-*Δ*pR_{ST98}. (C) PCR amplification of *spv*C (735 bp) gene. M: Axygen 2000 bp DNA ladder; lane 1: *S. typhi*-WT; lane 2: *S. typhi*-*Δ*pR_{ST98}; lane 3: *S. typhi*-c-pR_{ST98}; lane 4: pR_{ST98}/*E. coli* K12W1485.

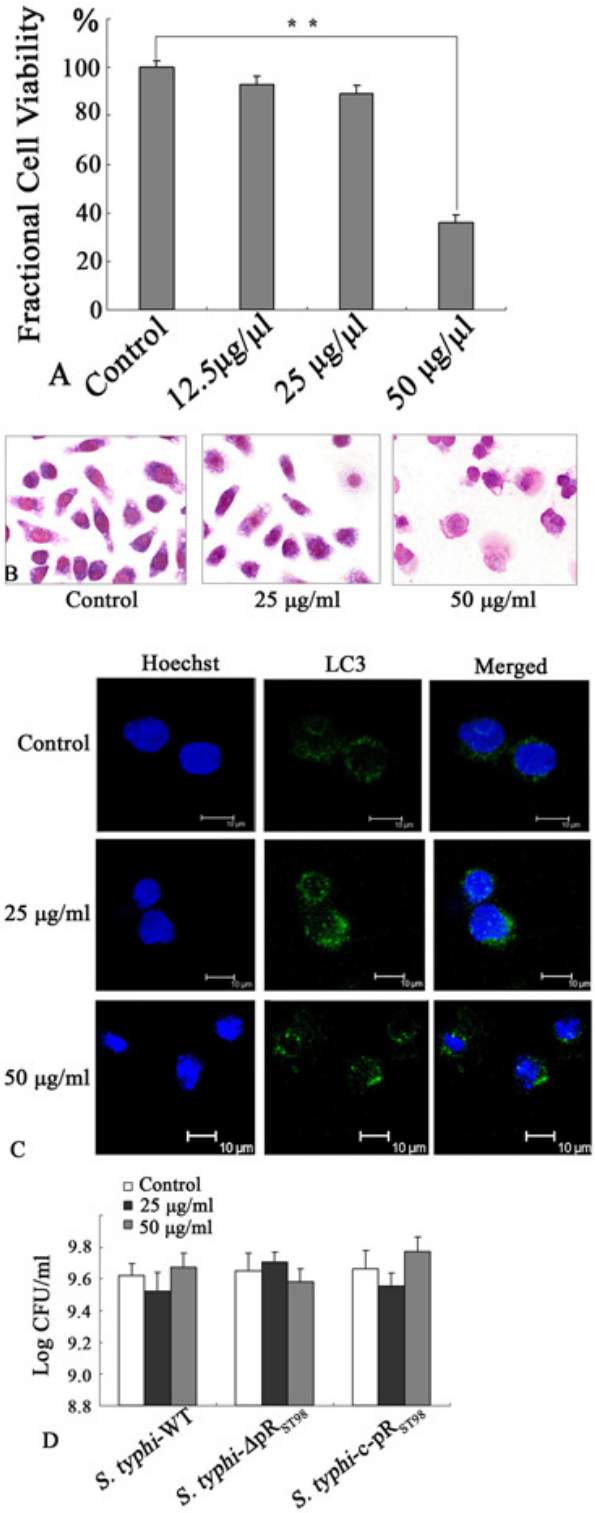

Figure 2. Determination of the optimal RAPA concentration. Exposure to RAPA for 24 h induced a concentration-dependent decrease in viability of J774A.1 macrophages (A), $^{**}P < 0.01$. After treating with different concentration of RAPA for 12 h morphological changes of J774A.1 macrophages were observed by Giemsa staining assay (B) and immunofluorescence (C). To visualize the autophagy vacuoles, cells were fixed and stained with anti-LC3 antibody. Bacteria survive after treating with different concentration of RAPA for 24 h (D). Bacterial Log colony-forming units per ml (y axis) were indicated.

staining cells showed that J774A.1 macrophages treated with 50 μg/ml RAPA for 12 h were obviously worse than the others. Cell membranes were damaged and there were few intact cells (Figure 2B).

As we known, RAPA acts as autophagy agonist and can activate autophagy. Compared with other pharmacy concentrations, immunofluorescence showed that there were obvious spot-fluorescent particles in J774A.1 macrophages cytoplasm treated with 25 μg/ml RAPA (Figure 2C). Serial dilution method and the test of OD values indicated that there ultrastructural level. In comparison with uninfected cells, 774A.1 macrophages treated with RAPA exhibited numbers of multivesicular structures. In the early period of infection (at 0-h time point), we observed a vacuolar compartment enclosing *S. typhi*-WT termed *Salmonella*-containing vacuole (SCV), while an autophagosome analogous double-membraned structure containing pathogens appeared inside cells infected with *S. typhi*-*Δ*pR_{ST98} (Figure 3A & 3E). After treatment of RAPA, autolysosome enclosing undigested pathogens and cytoplasmic contents were present in cells infected with *S. typhi*-WT at 2 h post-infection (Figure 3B & 3F).

Macrophage apoptosis appeared condensed and marginated nuclear chromatin. As shown in Figure 3C & 1G, J774A.1 macrophages infected with *S. typhi*-WT exhibited classical morphological features of apoptosis at 8 h post-infection. Numbers of intracellular pathogens were more in *S. typhi*-WT infected cells compared with that in *S. typhi*-*Δ*pR_{ST98} infected cells (Figure 3D & 3H).

4.4. Plasmid pR_{ST98} facilitates bacterial survival in J774A.1 cells

Two methods were used to measure bacterial survival. CFU obtained by cell lysis indicated that all strains increased viable counts during the whole 24 h infection process. Numbers of intracellular pathogens were significantly higher either in *S. typhi*-WT infected or *S. typhi*-c-pR_{ST98} infected cells compared with *S. typhi*-*Δ*pR_{ST98} for the first 12 h. After treated with RAPA, intracellular viable counts of *S. typhi*-WT decreased (Figure 4A). Bacterial survival in J774A.1 cells was also observed by Giemsa staining. At least 100 infected cells were enumerated in each group. There were less intracellular pathogens in *S. typhi*-*Δ*pR_{ST98} infected macrophages during the 24 h infection time frame, and significant difference among those groups could be found at 12 h post-infection (Figure 4B and 4C). At 24 h post-infection, most macrophages infected with *S. typhi*-WT or *S. typhi*-c-pR_{ST98} disintegrated. Results indicated that RAPA may decrease bacterial survival in the macrophages infected with *S. typhi*-WT and *S. typhi*-c-pR_{ST98} by activating of autophagy.

4.5. Plasmid pR_{ST98} inhibits LC3 labeling autophagy vacuoles in infected J774A.1 cells

As we known, mammalian autophagy protein LC3 is a marker of autophagic structures containing isolation membranes, autophagosomes and autolysosomes. Currently, a more reliable indicator of autophagic activity is the monitoring of LC3 turnover. This assay is based on extracting the membrane-unbound LC3-I form from cells and detect LC3-II, which is the membrane-associated form of LC3. Endogenous LC3-II is visualized by fluorescence microscopy as punctate structures that primarily represent autophagy vacuoles. It was demonstrated that *S. typhi*-*Δ*pR_{ST98} infected macrophages had more visible punctate LC3 structures compared with the other two groups at the early stage of infection (0-h time point). After interference with RAPA, there were obvious increasing numbers of punctate fluorescent particles in J774A.1 macrophages cytoplasm infected with *S. typhi*-WT and *S. typhi*-c-pR_{ST98} (Figure 5A).

Exploiting the difference of fluorescent proteins (mRFP, GFP) labeling LC3 can morphologically trace different stages of autophagy. When the low pH inside the lysosome quenches the fluorescent signal of GFP, mRFP-LC3 which exhibits more stable fluorescence in autolysosomes can readily be detected by fluorescence microscopy. Therefore, with this novel mRFP-GFP-LC3 tandem construction, autophagosomes and autolysosomes are labeled with yellow (i.e., mRFP and GFP) and red (i.e., mRFP only) signals, respectively (31). Transient transfection experiments indicated that *S. typhi*-*Δ*pR_{ST98} infected macrophages had more numbers of LC3 dots than *S. typhi*-WT infected cells at 0-h time point. After treated with RAPA, each group increased both in yellow LC3 dots (autophagosome) and red LC3 dots (autolysosome) (Figure 5B). Average numbers of punctate LC3 structures in at least 100 infected cells were shown in Figure 5C. More numbers of single red fluorescence signal were observed in macrophage cytoplasm infected with *S. typhi*-*Δ*pR_{ST98} than that in the other two groups indicated that *S. typhi* without R_{ST98} accelerated autophagic process. After interference with RAPA, LC3 punctate aggregation can be observed in macrophages infected with all strains.

4.6. Plasmid pR_{ST98} inhibits expression of autophagy protein LC-II and Beclin 1

This assay utilized flow cytometry to quantify the autophagosomal membrane-associated LC3-II. As shown in Figure 6A and 6B, mean fluorescence intensity of LC3-II expression in *S. typhi*-*Δ*pR_{ST98} infected macrophages was significantly stronger than that in the other two groups at 0-h time point, and RAPA increased the expression of LC3-II, but there was no significant difference among three groups.

Beclin 1, the mammalian orthologue of yeast Atg6, can participate in every major step in autophagic pathways, from autophagosome formation to autophagosome maturation. With a similar trend of LC3-II

4.3. Ultrastructure features of autophagy and apoptosis in J774A.1 cells infected with *S. typhi*

Electron microscopy is considered to be the gold standard for monitoring autophagic structures at the were no noticeable effects of each concentration of RAPA on the bacteria (Figure 2D). The treatment with RAPA no higher than 25 μg/ml has little effect on cellular responses, particularly protein synthesis, cellular metabolism and bacterial growth. As a result, 25 μg/ml RAPA was suitably used in this study.

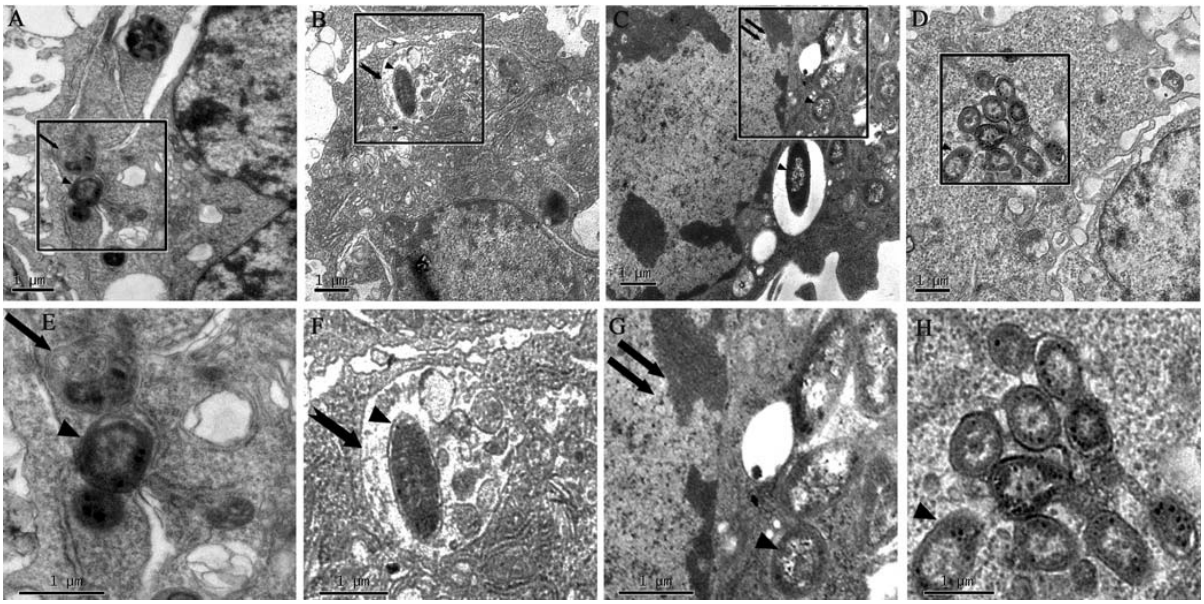

Figure 3. Transmission Electron Micrographs of Infected J774A.1 Macrophages. (A) J774A.1 cell infected with *S. typhi-Δ*pR$_{ST98}$ at 0-h time point. (B) RAPA pretreated J774A.1 cell infected with *S. typhi*-WT at 2 h post-infection. (C) Macrophage apoptosis caused by *S. typhi*-WT at 8 h post-infection. (D) *S. typhi*-WT replicates in J774A.1 cell. Boxed areas (E, F, G, and H) from A, B, C, and D are magnified respectively. (arrowheads, intracellular bacilli; arrows, autophagosomes; dovetail arrows, autolysosome; double arrows, marginated and condensed nuclear chromatin).

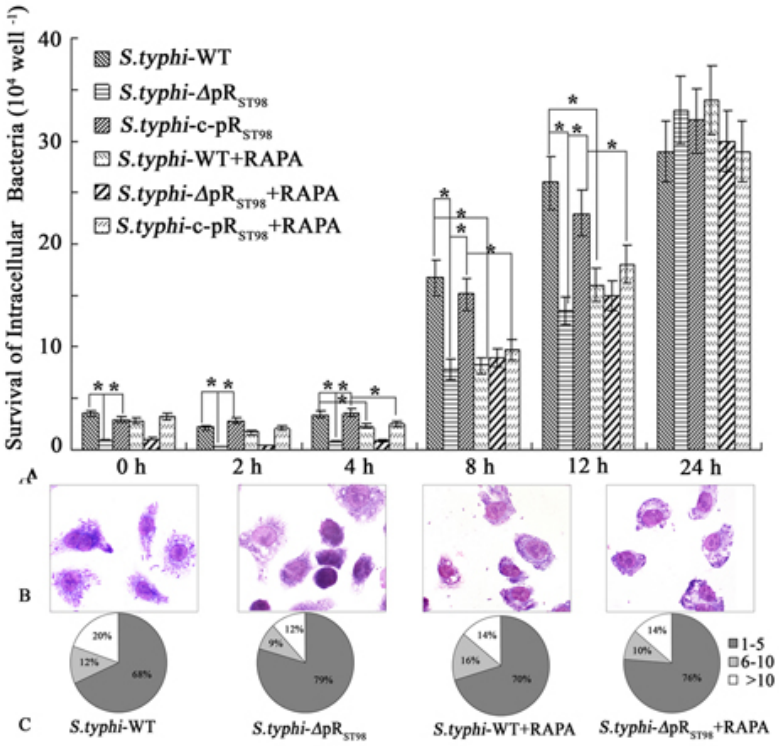

Figure 4. Numbers of Intracellular *Salmonella*. (A) Survival of intracellular bacteria was counted for each time point. The X axis represents hours post-infection and the Y axis represents 10^4 colony-forming units per well, $*P < 0.05$. (B) Bacterial survival in J774A.1 cells stained with Giemsa at 12 h post- infection. (C) The final number of intracellular bacteria was enumerated in at least 100 infected cells stained with Giemsa at 12 h post-infection.

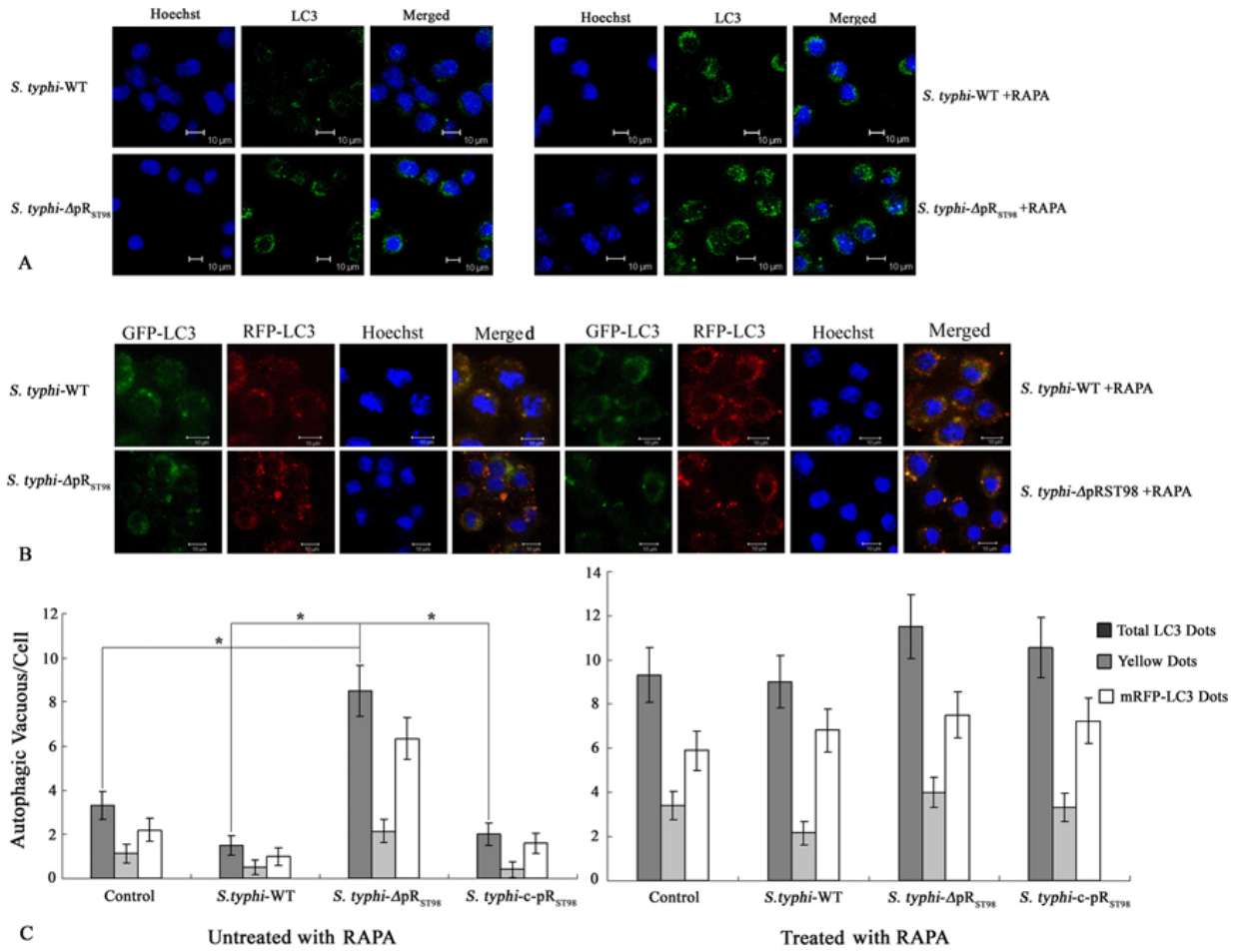

Figure 5. LC3 Puncta Formation Assays. (A) Macrophages infected with *S. typhi*-WT, *S. typhi -Δ*pR$_{ST98}$ respectively at 0-h time point were observed through immunofluorescence. (B) Macrophages transformants transiently expressing mRFP-GFP-LC3 were infected with *S. typhi*-WT, *S. typhi-Δ*pR$_{ST98}$ respectively at 0-h time point. (C) Punctate LC3 structures were enumerated by fluorescence microscopy. The average number of puncta was enumerated in at least 100 cells at 0-h time point, $*P < 0.05$.

expression, the difference of Beclin 1 expression appeared at 0-h time point and up-regulated after RAPA interference (Figure 6C and 6D).

4.7. Plasmid pR$_{ST98}$ promotes macrophage death through inhibiting autophagic activity

LDH is released into the culture medium following membrane broken as a result of either apoptosis or necrosis (32). As shown in Figure 7A, ratio of cell death measured by LDH release assay indicated no significant difference within 2 h post-infection. At 8 h post-infection, cell death ratio caused by *S. typhi-Δ*pR$_{ST98}$ was significantly lower than the other two groups. After treated with RAPA, cell death caused by *S. typhi*-WT decreased.

The relationship between plasmid pR$_{ST98}$ and macrophage apoptosis was further confirmed by flow cytometer analysis. It significantly suggested that more macrophage apoptosis was induced by *S. typhi*-WT and *S. typhi*-c-pR$_{ST98}$ than by *S. typhi-Δ*pR$_{ST98}$. Pretreated with RAPA resulted in a decrease in the level of apoptosis of macrophages infected with *S. typhi*-WT and *S. typhi*-c-pR$_{ST98}$, while plasmid free mutant infected cells had no significant change (Figure 7B and 7C).

Plasmid pR$_{ST98}$ causes caspase-3 dependent macrophage cell death. As shown in Figure 7D, caspase-3 activity of macrophages infected with *S. typhi*-WT was significantly higher than *S. typhi-Δ*pR$_{ST98}$ infected macrophages at 8 h post-infection, and RAPA could decrease caspase-3 activity. Results indicated that plasmid pR$_{ST98}$ could promote caspase-3 dependent apoptosis through inhibiting autophagic activity.

5. DISCUSSION

RAPA is a potent autophagy activator by targeting mTOR both *in vitro* and *in vivo (*31). Here we utilized RAPA to study the effect of plasmid pR$_{ST98}$ on the interaction between bacterial virulence and autophagy of macrophages J774A.1. Previous data demonstrated that pR$_{ST98}$ was related with the apoptosis of macrophages through the

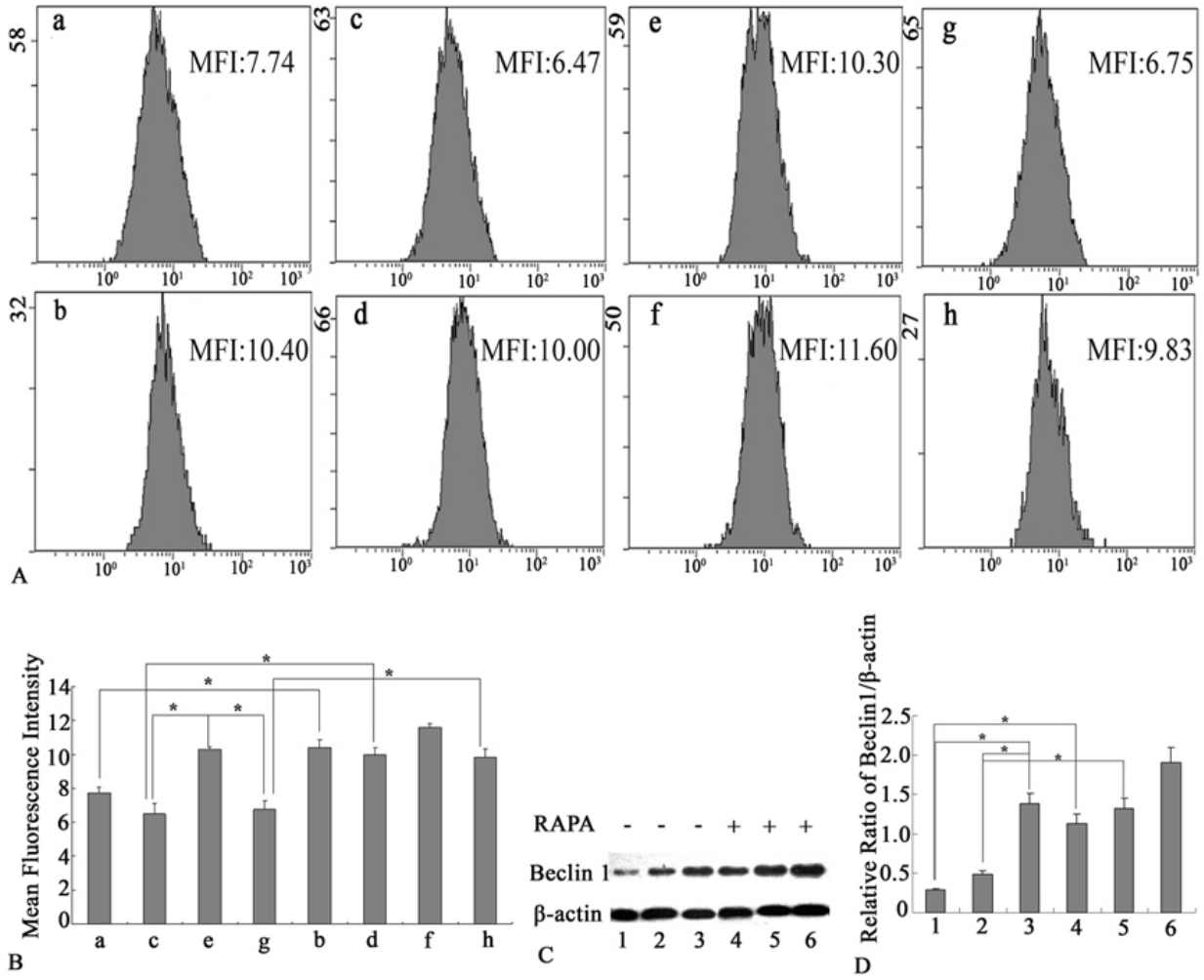

Figure 6. Detection of Autophagy Protein LC3-II and Beclin 1. (A and B) Quantification of autophagy protein LC3-II measured by flow cytometry at 0-h time point. Expression of LC3-II was positively correlated with mean fluorescence intensity (MFI). (a and b) uninfected cells; (c and d) J774A.1 cells infected with *S. typhi*-WT; (e and f) J774A.1 cells infected with *S. typhi*-*Δ*pR_{ST98}; (g and h) J774A.1 cells infected with *S. typhi*-c-pR_{ST98}. *S. typhi*-*Δ*pR_{ST98} infected macrophages displayed the highest mean fluorescence intensity (e) among the four groups without RAPA (a, c, e, and g). After RAPA interference mean fluorescence intensity of *S. typhi*-WT (d) and *S. typhi*-c-pR_{ST98} (h) group increased, $*P < 0.05$. (C) Expression of Beclin 1 in macrophages infected with *S. typhi*-WT, *S. typhi*-c-pR_{ST98} and *S. typhi*-*Δ*pR_{ST98} respectively at 0-h time point. Cells infected with *S. typhi*-WT, *S. typhi*-c-pR_{ST98}, and *S. typhi*-*Δ*pR_{ST98}, respectively (1, 2, and 3) and pretreated by RAPA(4, 5, and 6); (D) Semi-quantitative analyses of Beclin 1 expression based on the density of western blotting bands, $*P < 0.05$.

mitochondria pathway. Recently, Wei L *et al.* found its function in immune responses by restraining utophagy of DCs (8, 9), whether the plasmid affects macrophage autophagy is unknown. The inhibition of autophagy in *S. typhi*-WT infected macrophages was observed in this study; however, there remains the question as to what role pR_{ST98} plays in the relationship between autophagy and apoptosis. As described above, the relationship between autophagy and apoptosis is complicated. In recent studies we found that pR_{ST98}-induced cell apoptosis could be modulated by autophagy agonist RAPA, indicating that moderate autophagy was a strategy for macrophages to antagonize apoptosis induced by *S. typhi*.

Macrophages play an important role in *Salmonella* infections. The ability of residing and proliferation in macrophages is closely related to the strength of the *Salmonella* pathogenicity. The number of *S. typhi*-*Δ*pR_{ST98} in macrophages were significantly less than that of *S. typhi*-WT and *S. typhi*-c-pR_{ST98} for the first 12 h, confirming that pR_{ST98} promoted the bacterial survival in macrophages. After interference with RAPA, significant reduction could be seen in *S. typhi*-WT and *S. typhi*-c-pR_{ST98} groups, indicating that pR_{ST98} may enhance intracellular bacterial survival and RAPA-induced autophagy could restrict the growth of intracellular bacteria.

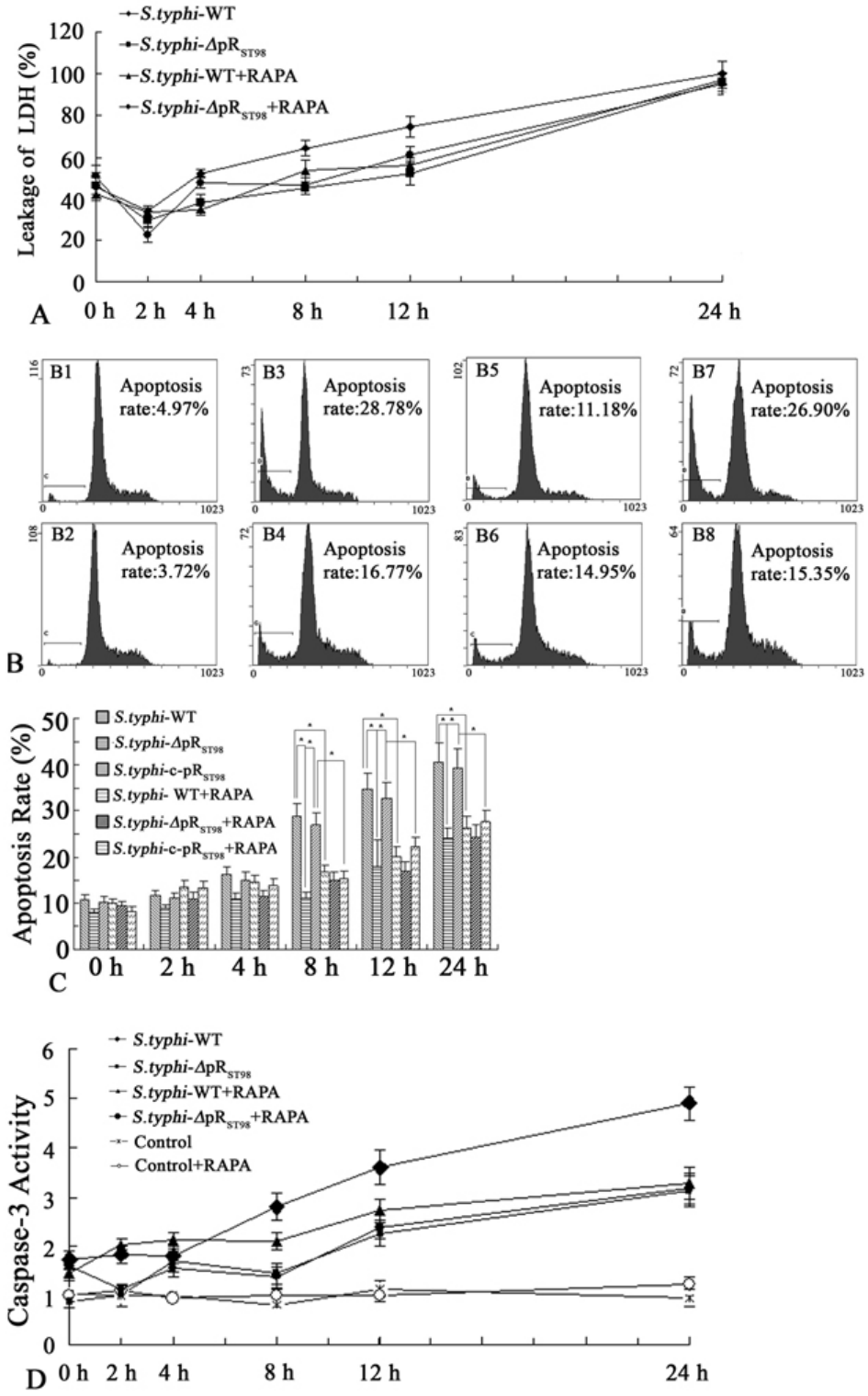

Figure 7. Assessment of cell death and apoptosis. (A) Assessment of cell death by measuring release rate of LDH into the culture media. (B) Assessment of apoptosis by measuring sub-diploid peak. (B1) uninfected cells; (B2) uninfected cells treated with RAPA; At 8 h post-infection, apoptosis rate of untreated (B3, B5, B7) and exposed to RAPA (B4, B6, B8) J774A.1 cells infected with *S. typhi*-WT, *S. typhi-Δ*pR$_{ST98}$, and *S. typhi*-c-pR$_{ST98}$, respectively; (C) Assessment of apoptosis over a 24 h infection time frame by flow cytometry, $*P < 0.05$. (D) Caspase-3 activities in culture supernatants of infected J774A.1 cells, $*P < 0.05$.

Autophagy was viewed until recently as a bona fide immunologic process with a wide array of roles in immunity. It defends eukaryotic cells against intracellular pathogens as a cell-autonomous innate defense. Many Atg proteins have been identified on the isolation membranes, including Beclin 1, LC3, Atg12, Atg13, ULK1/2, Atg16L1, Atg101, and FIP200. However, LC3 is the only Atg protein known to exist on complete autophagosomes, and therefore, this protein serves as a widely used marker for autophagosomes (31). It has been confirmed that LC3 directly catalyzed membrane hemifusionmembran-like process in the closing process, and inhibition of LC3 recruitment would increase the proliferation of *Salmonella* (33, 34). It was well known that during autophagy process, LC3-I protein conjugates to phosphatidylethanolamine to generate LC3-II, which is specifically associated with autophagosomal membranes. LC3-I is distributed in the cytosol, while LC3-II exhibits a punctate pattern when autophagy is induced. In this study, compared with *S. typhi*-WT and *S. typhi*-c-pR_{ST98} infected macrophages, there were more punctate fluorescent particles in macrophages infected with *S. typhi-Δ*pR_{ST98}. As autophagy is a dynamic process, two possibilities may explain for this. Either the plasmid pR_{ST98} inhibited the formation of autolysosome, or downstream of autophagy was exacerbated. Since the formation of autolysosome is contradictory to bacterial pathogenicity, we speculate that pR_{ST98} might involve in the upstream step of inhibiting autophagy. After interference with RAPA, red puncta (autolysosome) aggregation could be observed in *S. typhi*-WT and *S. typhi*-c-pR_{ST98} groups indicating that the autophagic degradation of intracellular bacteria was activated. These were consistent with the results obtained from the transmission electron microscope. Beclin 1 is a tumor suppressor gene and induces autophagy in mammalian cells. It may activate and bind with class III phosphoinositide-3-kinase to form the complex during the formation of autophagosome. In our study immunoblotting data showed that macrophages infected with *S. typhi-Δ*pR_{ST98} express the highest level of Beclin 1. After interference with RAPA, the expression of Beclin 1 was up-regulated. It was indicated that pR_{ST98} might down-regulate the expression of autophagy-associated protein. Collectively, our results revealed that pR_{ST98} may inhibite the autophagy of macrophages infected with *S. typhi*.

It was known that *Salmonella* might trigger caspase-3 mediated apoptosis in macrophages at certain stages of the pathogenic process (11). Caspase-3 was the primary executioner of apoptosis and the activity of caspase-3 in programmed cell death was irreversible. As been confirmed here, both *spv*B and *spv*C exist on pR_{ST98}, which were verified to be sufficient to confer plasmid-mediated virulence. It was well known that SpvB protein possessed ADP-ribosyl transferase activity to prevent the polymerization of G-actin monomer, resulting in the loss of F-actin filaments in infected macrophages. The loss of actin cytoskeleton led to the induction of host cell apoptosis through caspase-3 pathway (35). SpvC removed phosphate groups from host cell mitogen-activated protein kinases (MAPKs) to inactivate them thus blocking the downstream signaling pathways (36). MAPKs activated p38 MAPKs, which was essential for expression of anti-apoptosis proteins. In addition, p38 MAPKs signal pathways were involved in the expression of cytokines secretion such as NO, a trigger of autophagy (37, 38). Our study demonstrated that significantly stronger apoptosis of macrophages was induced by *S. typhi*-WT and *S. typhi*-c-pR_{ST98} than by *S. typhi-Δ*pR_{ST98}. After interference with RAPA, *S. typhi*-WT and *S. typhi*-c-pR_{ST98} groups resulted in a decrease in the level of apoptosis. The same trend could be seen in the activity of caspase-3, indicating that RAPA-induced autophagy seemed to inhibit the caspase-3 mediated apoptosis.

The above results revealed the effect of pR_{ST98} on bacterial virulence and the function of autophagy. *S. typhi* harboring pR_{ST98} displayed more virulence, triggering an increase in caspase-3-dependent apoptosis and cell injuries than pR_{ST98}-free strain by suppressing autophagy. Under these conditions, autophagy is a protective mechanism to lessen bacterial infection and improve cell survival. Autophagy inhibition may possibly be a self-protection mechanism by *S. typhi* harboring pR_{ST98} in order to avoid degradation. Macrophages infected with pR_{ST98}-free strain could resist the bacterial proliferation and remain vital by inducing moderate autophagy. After interference with RAPA, the suppressed autophagy in *S. typhi*-WT infected macrophages was activated, resulting in a certain protective effect. Unquestionably, autophagy will affect the infection process. We speculated that *spv* genes might be involved in regulation of host cell autophagy and apoptosis through the regulation of cytoskeleton and the p38 MAPKs signal pathways. Further molecule mechanisms and the signaling pathways involved in autophagy and apoptosis are definitely required to investigate. As a large plasmid containing complex sequences of unknown functions, it can't be excluded that other genes on pR_{ST98} may be co-involved in the process, thus full-gene sequencing and functional studies of the plasmid will be focused on during the further exploration.

6. ACKNOWLEDGEMENTS

ShuYan Wu and YuanYuan Chu contributed equally to this work. We are grateful to Prof Tamotsu Yoshimorim, Tokyo Medical and Dental University, Japan, for providing plasmid mRFP-GFP-LC3. We also thank Prof. Jie Yan, Zhejiang University, P. R. China, for providing murine macrophage-like cell line J774A.1. This study was supported by the Natural Science Foundation of P. R. China (No. 30972768), Special Research Fund for the Doctoral Program of High Education (No. 20103201110009), Natural Science Foundation of Jiangsu province (No. BK2011286), and sponsored by Jiangsu Overseas Research & Training Program for University Prominent Young & Middle-aged Teachers and Presidents.

7. REFERENCES

1. E Mweu, M English: Typhoid fever in children in Africa. *Trop Med Int Health* 13, 532-540 (2008)

2. T Butler. Treatment of typhoid fever in the 21st century: promises and shortcomings. *Clin Microbiol Infect* 17, 959-963 (2011)

3. JA Crump, ED Mintz: Global trends in typhoid and paratyphoid fever. *Clin Infect Dis* 50, 241-246 (2010)

4. DM Monack: Salmonella persistence and transmission strategies. *Curr Opin Microbiol* 15, 100-107 (2012)

5. CA Mayer, AA Neilson: Typhoid and paratyphoid fever-prevention in travellers. *Aust Fam Physician* 39, 847-851 (2010)

6. ZA Bhutta, J Threlfall: Addressing the global disease burden of typhoid fever. *JAMA* 302, 898-899 (2009)

7. MA Gordon, SM Graham, AL Walsh, L Wilson, A Phiri, E Molyneux, EE Zijlstra, RS Heyderman, CA Hart & ME Molyneux: Epidemics of invasive Salmonella enterica serovar enteritidis and S. enterica serovar typhimurium infection associated with multidrug resistance among adults and children in Malawi. *Clin Infect Dis* 46, 963-969 (2008)

8. R Huang, S Wu, X Zhang & Y Zhang: Molecular analysis and identification of virulence gene on pR (ST98) from multi-drug resistant Salmonella typhi. *Cell Mol Immunol* 2, 136-140 (2005)

9. Wei L, Wu S, Li Y, Chu Y & Huang R: Salmonella enterica serovar typhi plasmid impairs dendritic cell responses to infection. *Curr Microbiol* 65, 133-140 (2012)

10. S Wu, Y Li, Y Xu, Q Li, Y Chu, R Huang & Z Qin: A Salmonella enterica serovar typhi plasmid induces rapid and massive apoptosis in infected macrophages. *Cell Mol Immunol* 7, 271-278 (2010)

11. DG Guiney: The role of host cell death in Salmonella infections. *Curr Top Microbiol Immunol* 289, 131-150 (2005)

12. SL Fink. and BT Cookson: Pyroptosis and host cell death responses during Salmonella infection. *Cell Microbiol* 9, 2562-2570 (2007)

13. T Noda, S Kageyama, N Fujita & T Yoshimori: Three-axis model for Atg recruitment in autophagy against Salmonella. *Int J Cell Biol* 2012, 389562 (2012)

14. DJ Klionsky, SD Emr: Autophagy as a regulated pathway of cellular degradation. *Science* 290, 1717-1721 (2000)

15. L Galluzzi, O Kepp & G Kroemer: Autophagy and innate immunity ally against bacterial invasion. *EMBO J* 30, 3213-3214 (2011)

16. J Martínez-Borra1, C López-Larrea: Autophagy and self-defense. *Adv Exp Med Biol* 738, 169-184 (2012)

17. TL Thurston, MP Wandel, N von Muhlinen, F A oeglein & F Randow: Galectin 8 targets damaged vesicles for autophagy to defend cells against bacterial invasion. *Nature* 482, 414-418 (2012)

18. V Deretic: Autophagy in immunity and cell-autonomous defense against intracellular microbes. *Immunol Rev* 240, 92-104 (2011)

19. L Gong, RJ Devenish & M Prescott: Autophagy as a macrophage response to bacterial infection. *IUBMB Life* (2012)

20. K Kirkegaard, MP Taylor & WT Jackson: Cellular autophagy: surrender, avoidance and subversion by microorganisms. *Nat Rev Microbiol* 2, 301-314 (2004)

21. PH Rodrigues, M Bélanger, W Jr Dunn & A Progulske-Fox: Porphyromonas gingivalis and the autophagic pathway: an innate immune interaction? *Front Biosci* 13, 178-187 (2008)

22. CL Birmingham, JH Brumell: Methods to monitor autophagy of Salmonella enterica serovar typhimurium. *Methods Enzymol* 452, 325-343 (2009)

23. B CL irmingham, AC Smith, MA Bakowski, T Yoshimori & JH Brumell: Autophagy controls Salmonella infection in response to damage to the Salmonella-containing vacuole. *J Biol Chem* 281, 11374-11383 (2006)

24. S Shahnazari, WL Yen, CL Birmingham, J Shiu, A Namolovan, YT Zheng, K Nakayama, DJ Klionsky & JH Brumell: A diacylglycerol-dependent signaling pathway contributes to regulation of antibacterial autophagy. *Cell Host Microbe* 8, 137-146 (2010)

25. P Wild, H Farhan, DG McEwan, S Wagner, VV Rogov, NR Brady, B Richter, J Korac, O Waidmann, C Choudhary, V Dötsch, D Bumann & I Dikic: Phosphorylation of the autophagy receptor optineurin restricts Salmonella growth. *Science* 333, 228-233 (2011)

26. CA Collins, A De Mazière, S van Dijk, F Carlsson, J Klumperman & EJ Brown: Atg5-independent sequestration of ubiquitinated mycobacteria. *PLoS Pathog* 5, e1000430 (2009)

27. P Boya, RA González-Polo, N Casares, JL Perfettini, P Dessen, N Larochette, D Métivier, D Meley, S Souquere, T Yoshimori, G Pierron, P Codogno & G Kroemer: Inhibition of macroautophagy triggers apoptosis. *Mol Cell Biol* 25, 1025-1040 (2005)

28. MC Maiuri, E Zalckvar, A Kimchi & G Kroemer. Self-eating and self-killing: crosstalk between

autophagy and apoptosis. *Nat Rev Mol Cell Biol* 8, 741-752 (2007)

29. Y Xu, C Jagannath, XD Liu, A Sharafkhaneh, KE Kolodziejska & NT Eissa: Toll-like receptor 4 is a sensor for autophagy associated with innate immunity. *Immunity* 27, 135-144 (2007)

30. V Kaminskyy, A Abdi & B Zhivotovsky: A quantitative assay for the monitoring of autophagosome accumulation in different phases of the cell cycle. *Autophagy* 7, 83-90 (2011)

31. N Mizushima, T Yoshimorim & B Levine: Methods in mammalian autophagy research. *Cell* 140, 313-326 (2010)

32. F Vincenzi, M Targa, C Corciulo, S Gessi, S Merighi, S Setti, R Cadossi, PA Borea & K Varani: The anti-tumor effect of a (3) adenosine receptors is potentiated by pulsed electromagnetic fields in cultured neural cancer cells. *PLoS One* 7, e39317 (2012)

33. S Kageyama, H Omori, T Saitoh, T Sone, JL Guan, S Akira, F Imamoto, T Noda & T Yoshimori: The LC3 recruitment mechanism is separate from Atg9L1-dependent membrane formation in the autophagic response against Salmonella. *Mol Biol Cell* 22, 2290-2300 (2011)

34. H Nakatogawa, Y Ichimura & Y Ohsumi: Atg8, a ubiquitin-like protein required for autophagosome formation, mediates membrane tethering and hemifusion. *Cell* 130, 165-178 (2007)

35. SH Browne, P Hasegawa, S Okamoto, J Fierer & DG Guiney: Identification of Salmonella SPI-2 secretion system components required for SpvB-mediated cytotoxicity in macrophages and virulence in mice. *FEMS Immunol Med Microbiol* 52, 194-201 (2008)

36. P Mazurkiewicz, J Thomas, JA Thompson, M Liu, L Arbibe, P Sansonetti & DW Holden: SpvC is a Salmonella effector with phosphothreonine lyase activity on host mitogen-activated protein kinases. *Mol Microbiol* 67, 1371-1383 (2008)

37. Y Gao, W Jiang, C Dong, C Li, X Fu, L Min, J Tian, H Jin & J Shen: Anti-inflammatory effects of sophocarpine in LPS-induced RAW 264.7 cells via NF-KappaB and MAPKs signaling pathways. *Toxicol In vitro* 26, 1-6 (2012)

38. H Yuan, CN Perry, C Huang, E Iwai-Kanai, RS Carreira, CC Glembotski & RA Gottlieb: LPS-induced autophagy is mediated by oxidative signaling in cardiomyocytes and is associated with cytoprotection. *Am J Physiol Heart Circ Physiol* 296, H470-479 (2009)

Key Words: *Salmonella*, Plasmid, Autophagy, Apoptosis, Macrophage

Send correspondence to: Rui Huang, Medical College of Soochow University, No. 199, Ren Ai Road, Suzhou, Jiangsu 215123, P. R. China, Tel: 86-0512-65880132, Fax: 86-0512-65880103, E-mail: hruisdm@163.com